

STOCHASTIC ANALYSIS OF WIND TURBINE TOWERS WITH LUMPED MASS EFFECT AT THE TOP ON A FLEXIBLE FOUNDATION

Christoph W. T. Thiem^a, João A. P. Alves^b, Rubens Sampaio^b and Peter Hagedorn^c

^a *Technische Universität Darmstadt, Institute of Numerical Methods in Mechanical Engineering and Graduate School Computational Engineering, Dolivostr. 15, D-64293 Darmstadt, Germany*
<http://www.fnb.tu-darmstadt.de> (thiem@fnb.tu-darmstadt.de)

^b *Pontifícia Universidade Católica do Rio de Janeiro, Rua Marquês de São Vicente, 225 - Gávea - RJ - Brazil* <http://www.puc-rio.br> (piresalves.ja@gmail.com; rsampaio@puc-rio.br)

^c *Technische Universität Darmstadt, Dynamics and Vibrations Group, Institute of Numerical Methods in Mechanical Engineering, Dolivostr. 15, D-64293 Darmstadt, Germany*
<http://www.dyn.tu-darmstadt.de> (peter.hagedorn@dyn.tu-darmstadt.de)

Keywords: Structural dynamics, Mechanical design, Structural Reliability, Propagation of uncertainties, Eolic energy.

Abstract. A wind turbine is an example of multidisciplinary engineering fields. In order to construct high efficient and resistant turbines, preliminary analysis are necessary in several different fields. The most obviously needed investigation is the fluid-structure interaction but a correct analysis of the soil characteristics is also important. Turbines are subjected to wind and sea wave loadings, both random. So, it makes sense to design the structures using a random approach in order to associate to the structure a probability of failure. In this paper, the characterization of the dynamic behavior of a specific type of those structures are presented and discussed, considering the free vibration analysis (modal analysis), incorporating lumped mass and foundation effects. The analysis is made using both variational and strong formulations. In both approaches, some specific properties are chosen as random. Monte Carlo and collocation methods are used as the base to check out the effectiveness of the Finite Element algorithm.

1 INTRODUCTION

Wind power generation became an important activity nowadays because, besides being a clean and renewable source of energy, it is getting more and more attractive from the economic point of view even in places where other energetic resources are abundant.

Nowadays, maybe the most common configuration of a wind turbine is that composed by a tower with a generator installed at its top, actuated by a horizontal shaft as sketched at Figure 1. The rotor configuration varies but the most common is the three-bladed.

The towers are in general made with a very high slender tube and they are installed on- and off-shore (always to take advantage of the better conditions of the wind).

Attention must be paid to the foundation where the structure of the turbine is going to be placed because the installation characteristics can affect its dynamic behavior (Adhikari and Battacharya (2012)). Figure 1 shows some configurations used in bottom-mounted-off-shore turbines installation.

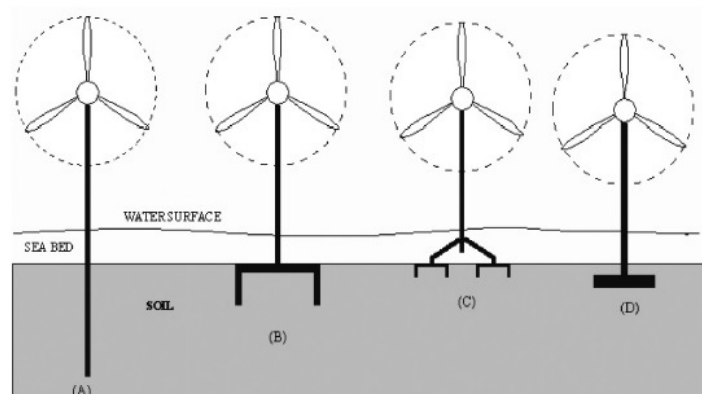


Figure 1: Off-shore configurations (Adhikari and Battacharya (2012))

2 TOWER MODEL: EQUATION OF MOTION AND BOUNDARY CONDITIONS

A beam with bending stiffness $EI(x)$, mass per unit length $m(x)$ and radius of gyration of the cross section $r(x)$ is installed in a supporting structure so that its base is permitted to rotate and move laterally, as shown in Figure 2. This can be modeled using translational and rotational springs at the base, k_l and k_r (Adhikari and Battacharya (2012)). The two springs simulate the interaction between the tower and the top of a pillar, where is installed the tower. The behavior of the pillar will depend on the soil characteristics.

The beam has a body installed at its top whose mass and rotational inertia are M_n and J_n , respectively. In general, in a 2D model, the beam is modeled as subjected to two kind of loads. One vertical, $P(x)$ and other horizontal and distributed, $f(x, t)$. $P(x)$ is due to the weights of both, nacelle and part of the tower which is above the coordinate x (where $P(x)$ is evaluated), as well as to the force caused by any unbalance of the rotor due to imperfections in blades assembling (in general harmonic, whose frequency is denoted by $1P$). In this work, it is not considered the influence of the tower weight in $P(x)$, neither the unbalance effect. It is considered that $P(x) = P(L) = M_n g$; g is the gravitational acceleration.

$f(x, t)$ is due to the wind and waves. Considering the wind action, when passing through the plane of the rotation, it causes torques and forces on the blades which are transmitted to the structure. Another important effect is also caused by the blades when they pass in front of the

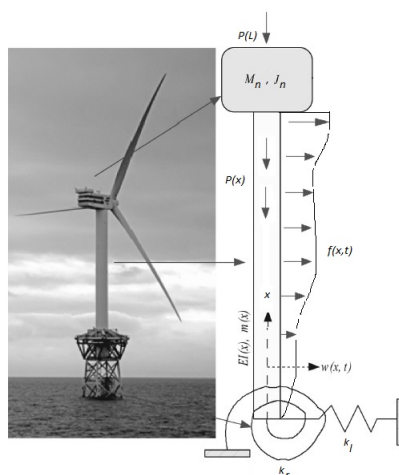


Figure 2: Tower and its simplified model (Adhikari and Battacharya (2012))

tower with a frequency of nP (n is the number of blades) (Tempel and Molenaar (2002)). One has to make sure that those two loading frequencies ($1P$ and nP) do not coincide with any of those of the structure. Often, the first natural frequency is considered as the primary indicator of the dynamic responses (Adhikari and Battacharya (2012)). This means that the response of the structure in frequency must be known to ensure a safe design.

The differential equation which models the tower as an Euler-Bernoulli beam under the conditions presented is well known and can be found in literature, (Adhikari and Battacharya (2012), Inman (2003) and Meirovitch (1997)) and is presented below:

$$\frac{\partial^2}{\partial x^2} \left(EI(x) \frac{\partial^2}{\partial x^2} w(x,t) \right) + \frac{\partial}{\partial x} \left(P(x) \frac{\partial}{\partial x} w(x,t) \right) - \frac{\partial}{\partial x} \left(m(x)r(x)^2 \frac{\partial}{\partial x} \dot{w}(x,t) \right) + m(x)\ddot{w}(x,t) = f(x,t) \quad (1)$$

with boundary conditions for $x = 0$,

$$\begin{aligned} \sum F_0(0,t) &= k_t w(0,t) \\ \sum M_0(0,t) &= k_r \frac{\partial}{\partial x} w(0,t) \end{aligned} \quad (2)$$

and for $x = L$

$$\begin{aligned} \sum F_L(L,t) &= M_n \ddot{w}(L,t) \\ \sum M_L(L,t) &= J_n \frac{\partial}{\partial x} \dot{w}(L,t) \end{aligned} \quad (3)$$

where F_0 , M_0 , F_L , and M_L are the forces and torques at the positions $x = 0$ and $x = L$ and no essential conditions are imposed. For initial conditions one has $w(x,0) = w_0(x)$ and $\dot{w}(x,0) = \dot{w}_0(x)$.

2.1 Variational formulation

In variational formulation, the differential equation is multiplied by a chosen function $\psi(x)$ and integrated over the domain.

For the present case, after integration, the variational formulation becomes

$$\begin{aligned}
 & M_n \ddot{w}(L, t) \psi(L) + J_n \frac{\partial}{\partial x} \ddot{w}(L, t) \psi(L) dx + k_t w(0, t) \psi(0) + \\
 & k_r w(0, t) \frac{\partial}{\partial x} w(0, t) \psi(0) + \int_0^L EI(x) \frac{\partial^2}{\partial x^2} w(x, t) \frac{d^2}{dx^2} \psi(x) dx \\
 & - \int_0^L P(x) \frac{\partial}{\partial x} w(x, t) \frac{d}{dx} \psi(x) dx + \int_0^L mr^2(x) \frac{\partial}{\partial x} w(x, t) \frac{d}{dx} \psi(x) dx \\
 & - \int_0^L f(x, t) \psi(x) dx = 0
 \end{aligned} \tag{4}$$

$$\forall \psi(x) : [0 \ L] \longrightarrow \Re / \psi(x) \in C^2; \int_0^L \psi^2(x) < \infty.$$

To obtain the Equation 4, the following boundary conditions were considered:

$$\begin{aligned}
 & \frac{\partial}{\partial x} \left[EI(L) \frac{\partial^2}{\partial x^2} w(L, t) \right] + P(L) \frac{\partial}{\partial x} w(L, t) \\
 & - mr^2(L) \frac{\partial}{\partial x} \ddot{w}(L, t) = M \ddot{w}(L, t)
 \end{aligned} \tag{5}$$

and

$$\begin{aligned}
 & - \frac{\partial}{\partial x} \left[EI(0) \left(\frac{\partial^2}{\partial x^2} w(0, t) \right) \right] - P(0) \frac{\partial}{\partial x} w(0, t) \\
 & + mr^2(0) \frac{\partial}{\partial x} \ddot{w}(0, t) = k_t w(0, t).
 \end{aligned} \tag{6}$$

In the same way

$$-EI(L) \frac{\partial^2}{\partial x^2} w(L, t) = J_n \frac{\partial}{\partial x} \ddot{w}(L, t) \tag{7}$$

and

$$EI(0) \frac{\partial^2}{\partial x^2} w(0, t) = k_r \frac{\partial}{\partial x} w(0, t). \tag{8}$$

In finite element discretization, the equation 4 must hold in each element. Using Galerkin method, the elemental equations are used to obtain a system of equations in terms of global coordinates in the form

$$[\mathbf{M}] \ddot{\mathbf{w}} + [\mathbf{K}] \mathbf{w} = \mathbf{f}, \tag{9}$$

For bending displacement, for instance,

$$w_i(x, t) \sim \sum_1^N \bar{w}_{ij}(t) \phi_j(x), \tag{10}$$

where, $w_i(x, t)$ is the deflection function in direction i , $\bar{w}_{ij}(t)$ is the j - th nodal displacement in direction i and $\phi_j(x)$, the j - th interpolation function ($i = 1, 2, 3; j = 1, \dots, N$). $[\mathbf{K}]$ and $[\mathbf{M}]$ are the stiffness and mass matrices. In this work, the interpolation functions $\phi_i(x)$ are chosen

as Hermitian beam element functions with two-node per element. Considering external forces null, the modal alternative to Equation 9 can be obtained as

$$[\mathbf{K} - \omega^2 \mathbf{M}] \mathbf{w} = \mathbf{0}, \quad (11)$$

where ω^2 are the N eigenvalues of the problem. The solutions obtained for the equation (11) gives a finite number of eigenvalues ω_i^2 and their respective eigenvectors Φ_i , ($i = 1, 2 \dots N$). This is an approximation for the solutions of the problem and as the number of the finite elements increases, more eigenvalues are found and closer the solution of the equation (11) gets to the solution of the problem.

2.2 Strong formulation

In strong formulation, the differential equation (1) is solved directly using separation of variables technique. For constant geometric and constitutive parameters, the modes are the solution for equation

$$\frac{d^4 w(\xi)}{d\xi^4} + \tilde{\nu} \frac{d^2 w(\xi)}{d\xi^2} - \Omega^2 w(\xi) = p(\xi). \quad (12)$$

Notice that it is in a non-dimensional form (Adhikari and Battacharya (2012), Wu and Hsu (2006)) whose non-dimensional parameters are defined as $\xi = \frac{x}{L}$, $\nu = \frac{P(L)L^2}{EI}$, $\Omega^2 = \omega^2 \frac{mL^4}{EI}$, $\mu = \frac{r}{L}$, $\tilde{\nu} = \nu + (\mu\Omega)^2$, $\eta_r = \frac{k_r L}{EI}$, $\eta_l = \frac{k_l L^3}{EI}$, $\alpha = \frac{M_n}{mL}$ and $\beta = \frac{J_n}{mL^3}$. $p(\xi)$ is the non-dimensional distributed loading and ω , the natural frequencies. The boundary conditions for bending moment and shear force at $\xi = \frac{x}{L} = 0$ are equivalent to those already presented

$$\frac{d^2 w(0)}{d\xi^2} - \eta_r \frac{dw(0)}{d\xi} = 0, \quad \frac{d^3 w(0)}{d\xi^3} + \tilde{\nu} \frac{dw(0)}{d\xi} + \eta_l w(0) = 0. \quad (13)$$

and at $\xi = 1$,

$$\frac{d^2 w(1)}{d\xi^2} - \beta \Omega^2 \frac{dw(1)}{d\xi} = 0, \quad \frac{d^3 w(1)}{d\xi^3} + \tilde{\nu} \frac{dw(1)}{d\xi} + \alpha w(1) = 0. \quad (14)$$

For a modal analysis, first the external load is made null. Then, the solution of the equation is supposed to be $w(\xi) = e^{\lambda\xi}$ and substituting it into Equation (12), the general solution for the modes is obtained:

$$w(\xi) = b_1 \sin(\lambda_1 \xi) + b_2 \cos(\lambda_1 \xi) + b_3 \sinh(\lambda_2 \xi) + b_4 \cosh(\lambda_2 \xi) \quad (15)$$

where $\lambda_{1,2} = \lambda_{1,2}(\nu, \mu, \Omega)$. The parameters b_i , $i = 1$ to 4, are determined imposing the boundary conditions 13 and 14, which leads to a 4×4 system of algebraic equations

$$\mathbf{Rb} = \mathbf{0} \quad (16)$$

where $\mathbf{b} = [b_1, b_2, b_3, b_4]^T$. The components of \mathbf{b} depend on the non-dimensional parameters presented above. For a nontrivial solution, $\det[\mathbf{R}] = 0$, so, one has to look for values of Ω that are solutions of equation (16), for a given set of properties. A comprehensive analysis for this can be found in Adhikari and Battacharya (2012).

3 RANDOM SIMULATIONS

3.1 Theory of uncertainty

In physical problems often not all parameters are precisely known. Reasons for such uncertainties can be e.g. natural fluctuations, fabrication tolerances or the lack of knowledge. In safety-relevant applications it may be necessary to take into account these uncertainties, for example to comply the Six Sigma criterion. For this purpose, uncertain input parameters like geometric dimensions, material parameters, forces or boundary conditions, have to be modeled as random parameters. The substitution of input parameters by random variables leads to a system output which cannot be described by a single value anymore but by a distribution of probabilities associated to that value like shown in Figure 3.

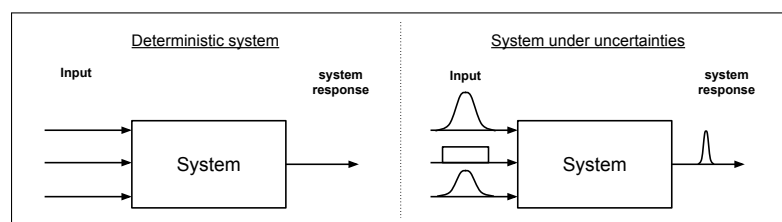


Figure 3: Comparison: System response with(right) and without(left) uncertainty

The resulting system, which also is called stochastic problem, can be solved e.g. with non intrusive methods (Le Maître and Knio (2010)) which means to solve a set of deterministic problems. In this paper it was decided to use the widespread Monte-Carlo method as well as the more efficient adaptive stochastic collocation method on sparse grids, to solve the stochastic problem. In the following the latter method is explained. The algorithm is based on the work of Schieche (2012). As the name indicates, this method is based on collocation points. These points represent possible realizations of the random input parameters. Since these are explicit values, it is possible to simulate this realization of the model with a common deterministic solver. The following is a brief overview of the steps of the algorithm operation:

1. Choose a set of collocation points on a sparse grid.
2. Solve for each collocation point the corresponding deterministic problem.
3. Interpolate the solutions in order to get a continuous representation of the random solution field.
4. Estimate statistical quantities based on the means of adequate quadrature rules.
5. Calculate the interpolation error and if needed add collocation points.

The nested quadrature nodes of Clenshaw-Curtis or Gauss-Patterson cubature (Schieche (2012)) is used in order to chose the collocation points. Once the deterministic problems are solved, the interpolation is done via a global, hierarchical basis interpolation. The aspect of the hierarchy allows the use of hierarchical surpluses as error indicators. These error indicators are needed in order to adaptively control the number of collocation points. This method is proposed and described in Gerstner and Griebel (2003). The implementation of this scheme as well as the analytical simulation of the beam from Chapter 2 is written in MATLAB.

A real case is simulated whose characteristics are presented in Table 1.

Dimensional parameters	Values
Length (L)	55 m
Average diameter (D)	3.37 m
Thickness (t_h)	0.0068 m
Mass density (ρ)	7860 kg/m ³
Young's modulus (E)	210 GPa
Top mass (M_n)	35700 kg
Non-dimensional parameters	Values
Axial force ν	0.049
Lateral foundation stiffness (η_l)	40.02
Rotational foundation stiffness (η_r)	5935
Mass ratio (α)	1.15
Radius of gyration (μ)	≈ 0
Rotary inertia (β)	0

Table 1: Turbine properties and parameters (Adhikari and Battacharya (2012))

3.2 Stochastic model

For the identification of the most influential parameters that should be treated as uncertain for further calculation one refers firstly to the results of Adhikari and Battacharya (2012) and the other hand on the analysis of variance which is proposed by Harzheim (2008). The former leads to that we handle the rotational and lateral foundation stiffnesses as uncertain. Besides the notable influence to the natural frequency, these parameters can only be calculated approximately what inevitably leads to discrepancies with the real model and thus represents a source of uncertainty.

As mentioned above the remaining input parameters from Table 1 are examined with an analysis of variance. The method described in 3.1 can estimate how the variance of the system output is composed of the input variances. A detailed explanation would exceed the scope of the work therefore one refers to the work of Harzheim (2008), Jeong et al. (2004) and Jones et al. (1998). At this point, only a crude description is given. The aim of this method is to determine the relative influence σ_i of each uncertain parameter on the total variance σ_{tot}^2 of the system. For this purpose the quantities σ_i are calculated using a breakdown of the function $y(\vec{x})$ into a sum of single factors similar to Taylor series. Based on these values σ_i it can be decided which parameters should be treated as uncertain and which are not.

The expense of an analysis can be justified by the fact that one performs many different calculation for the further stochastic analysis so that the initial overhead can be compensated. The analysis of variance is performed with the first six quantities from Table 1, L , D , t_h , ρ , E , M_n . Even the rotational and lateral foundation stiffness is already announced to be treated as uncertain they have to taken into account for this analysis in order to achieve an adequate comparison. In this method, a set to uniform distribution is used with relative large fluctuation (Harzheim (2008)). The chosen quantity of fluctuations is based on certain specifications of the parameters. For example, the value of the density varies $\pm 3\%$ around its given mean value since this is a common tolerance (HeidelbergCementAG (2011)). Similarly the length of the beam diversifies by $\pm 1\%$ although this is probably over the top for a tower with such a large height compared to the given tolerance in Schöwer (2013). For the mass M_n , diameter D and thickness t_h the distribution extends from -5% to $+5\%$ because these values are rounded and

based on simplifications. The remaining quantities, k_l , k_r and E , can only be roughly estimated, so this justifies the large distribution of $\pm 10\%$.

The analysis is run four times with different values for the mean of k_r and k_l in order to get an overview of the impact of different realizations of the foundation of the wind turbine. The results are shown in Figure 4 for the most important variations (E , D , η_r (or k_r) and η_l (or k_l)). All the others maximum values are below 12%.

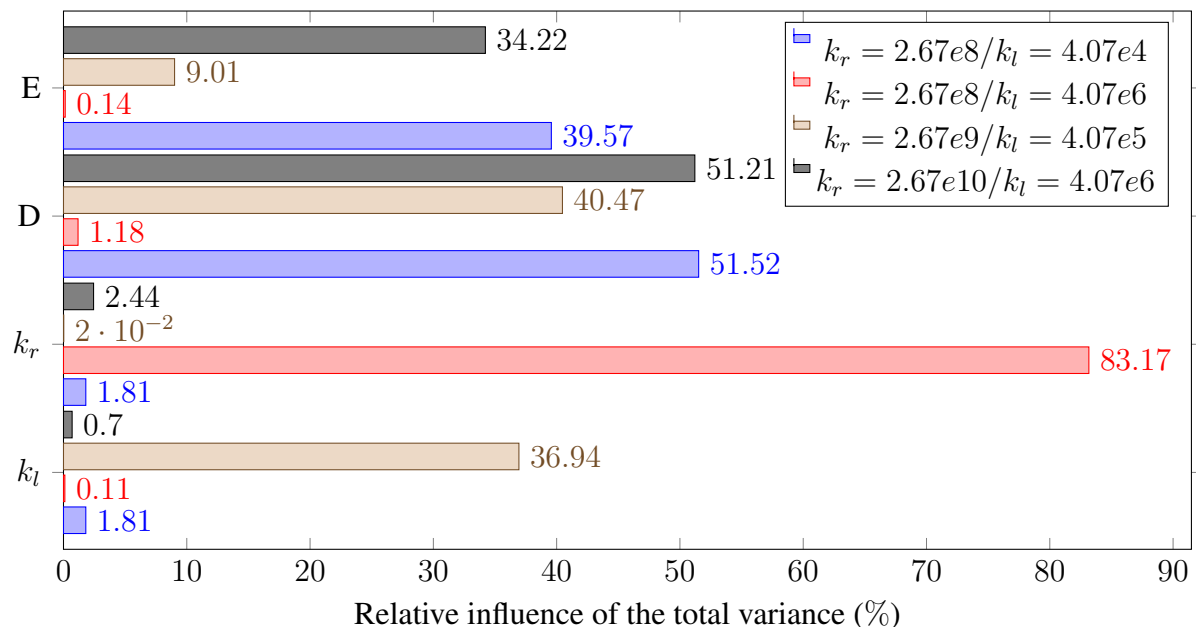


Figure 4: Analysis of variance of all input parameters

It is noticeable that the results of the analysis of variance depend highly on the given values of the foundation stiffnesses parameters k_l and k_r . It must be considered that their determination for real cases is somehow indirect and sometimes based on experimental approach (Adhikari and Battacharya (2012)) and for this reason, these parameter will be treated as random variables.

Figure 4 shows that the parameters E and D can also have a large relative influence on the variance. In further work, these parameters must be taken into account. But for the operation points that are examined in this work it is not necessary. Therefore, these parameters are treated for simplifying and enhance comparability as deterministic.

Now, the soil parameters are not deterministic anymore and they are better represented by two random variables, say, X_{k_l} and X_{k_r} , with support $[0.9k_l \ 1.1k_l]$ and $[0.9k_r \ 1.1k_r]$, respectively. In the same way, the non-dimensional parameter associated also are random variables X_{η_l} and X_{η_r} , with support $[0.9\eta_l \ 1.1\eta_l]$ and $[0.9\eta_r \ 1.1\eta_r]$, respectively, with expectations $E\{X_{\eta_l}\} = \eta_l = 40.02$ and $E\{X_{\eta_r}\} = \eta_r = 5935$ (from Table 1), respectively.

The joint-PDF for those two random variables is not known, but it is reasonable suppose that values for those two parameters were obtained in an independent way, the random variables X_{η_l} and X_{η_r} can be considered statistically independent. With this level of information, it is advisable to choose a distribution that, recalling Shannon (theorem of Maximum Entropy), maximizes the uncertainty. So, in this case, the uniform distribution is the one.

4 RESULTS

The idea here was to solve the problem proposed in terms of modal analysis and investigate the influence of the random behavior of the two so called soil-structure interaction parameters, k_l and k_r (or equivalently, η_l and η_r), in the natural frequencies and modes random responses. In order to obtain the approximation for the problem, that is, the approximated random modal responses and respective natural frequencies, the two formulations described above, namely the strong (based on equations 15 and 16), approach A, and variational (following the methodology described in 2.1), approach B, were codified and simulated. Monte Carlo was used for the random analysis for both approaches.

In order to validate the codes, a third program based on collocation was adapted to this specific case. The three codes were developed in MATLAB.

In all simulations, the two soil-structure interaction parameters are considered as represented by two random variables although one must recall that all turbine geometric and constitutive properties are considered constant in x and t .

Next it will be presented the results for simulations. In all graphs are depicted a histogram and an adjusted probability density function. Both graphic renditions contain nearly the same information, but the histogram provides the real non-smoothed data while the PDF is more suitable for the visualization of the qualitative characteristics of the probability density.

In the reference [Adhikari and Battacharya \(2012\)](#), data from a real turbine are presented and some are used here. In that work, average values are given for three real turbines together with the complete set of non-dimensional parameters and their respective measured and predicted 1st natural frequencies. One of those sets, turbine "Irene Vorrink", has the non-dimensional parameters: $\nu = 0.030$, $\eta_l = 39.64$, $\eta_r = 5880$, $\alpha = 1.144$, $\beta = 0$ and $\mu \sim 0$. The 1st natural frequency is 0.4565 Hz. Using those non-dimensional parameters given, comparison was possible using approach A, directly. However, when using approach B, some dimensional data have to be calculated (e.g., diameter, length, thickness etc) from information available and some parameters got quite different, e.g., the loading parameter ν became 75% larger in present work, making the structure softer than that of the reference paper. Just to validate the results, the set of parameters above was used under approach A, with collocation method and the results are presented in Figure 5 that shows the first natural frequency distribution for a tolerance of $1.0 \cdot 10^{-5}$ and a maximal number of interactions of 30, for 11 collocation points. The global error indicator was $4.2 \cdot 10^{-8}$ and the largest local error indicator was $4.3 \cdot 10^{-8}$.

It is observed in Figure 6 that the same results are obtained using Monte Carlo simulation. Also, the mean value is the same for the two simulations and in accordance with that results obtained in [Adhikari and Battacharya \(2012\)](#) (1st natural frequency 0.4565 Hz). The CPU time spent for solving the problem in the case of the 1st mode using Monte Carlo simulation is smaller than that spent in simulations using collocation method as can be seen in Table 2. It was used a machine with 2GHz Intel Core i7, 8Gb (64b running Windows 8 SL). Although not making comparison between the two methodologies for higher modes, the CPU time spent on using Monte Carlo for simulation for 4th and 5th modes is too long. More simulations have to be carried out in order to compare more modes in both methodologies aiming a more solid conclusion, but due to the conception of the code for finding the roots of the equation 16, for each realization, the program must find all the natural frequencies up to the maximum value required. Improvements must be made in the program in order to look for the roots in a more efficient way, reducing the computational time. This was to compare both collocation and Monte Carlo algorithm under the strong formulation.

The non-dimensional values presented on the Table 1 were calculated considering the information given in Adhikari and Battacharya (2012). With the information available those parameters got quite different and the natural frequencies got smaller than that obtained in the reference. That is mainly because the parameter ν calculated here is about 75% larger. The parameters η_r and η_l also increase but in a smaller relative amount. The Figures 7 and 8 show the distribution of the 1st natural frequency and for the amplitude of the 1st mode for a specific point of the beam ($\xi = 0.75$ or 75% of the total length). It is interesting to notice that, not considering the slope, the graphs keep some uniform characteristics. The next two Figures, 9 and 10, depict the results for the natural frequencies and amplitude of the 4th mode (at $\xi = 0.75$). The two graphs in Figures 11 and 12, represent the same as in the previous figures but the shape is different, quite triangular. The influence of the parameter η_l is more important for smaller natural frequencies in this turbine configuration. That is why the form of the resultant distribution keeps some uniform characteristics. For larger natural frequencies, the presence of the rotational spring (parameter η_r) becomes more important and the combination of both uniform distributions leads to a quite triangular resultant distribution for the 5th natural frequency (as presented in the respective graph) and becoming bell shaped for even larger natural frequencies. For obtaining the graphs presented in that figures, it took about 7min and that was the longer time.

The graphs of the Figures 13, 14 and 15 show all the realizations for each mode within a probability of 98%. As can be observed, the curves resultant of each realization are almost coincident. This means that the modes are low sensitive to uncertainties in parameters considered, for this specific turbine. It can also be observed in the magnitude of the standard deviations, that is very small.

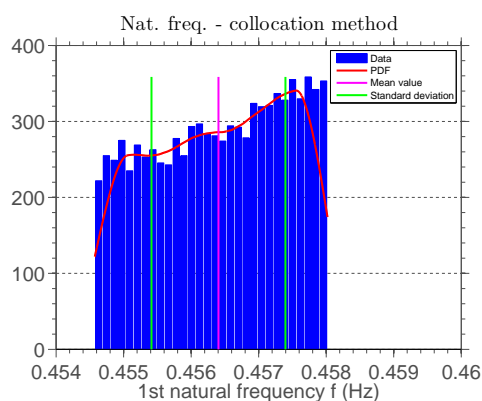


Figure 5: 1st natural frequency Collocation (param. as in Adhikari and Battacharya (2012))

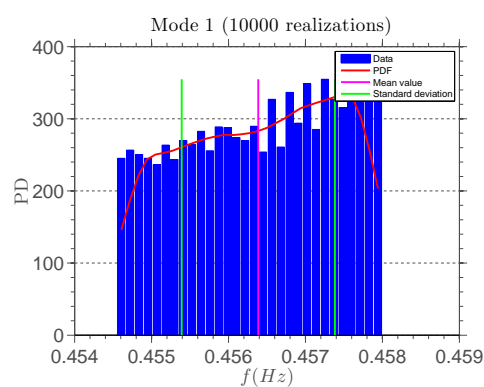


Figure 6: 1st natural frequency Monte Carlo (param. as in Adhikari and Battacharya (2012))

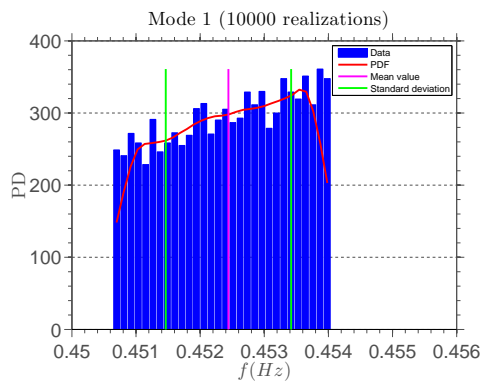


Figure 7: PDF - 1st natural frequency (calcul. param.)

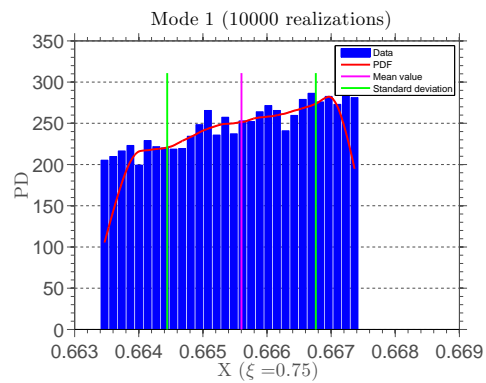


Figure 8: PDF - 1st mode ($\xi = 0.75$)

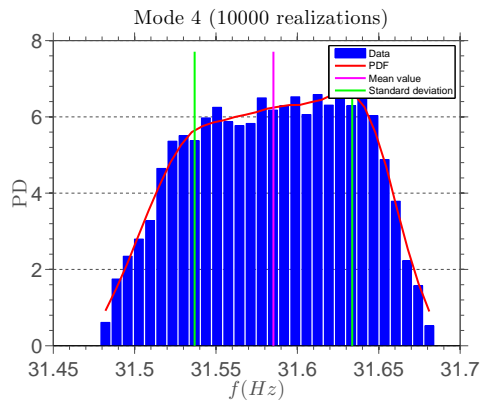


Figure 9: PDF - 4th natural frequency (calcul. param.)

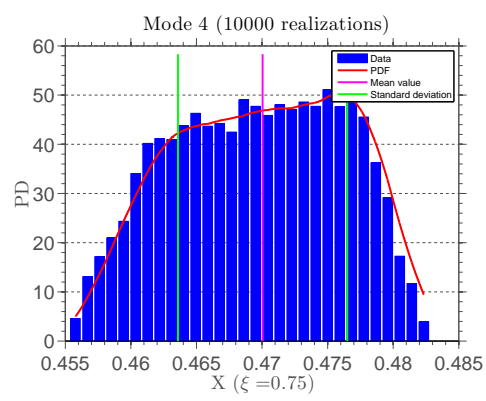


Figure 10: PDF - 4th mode ($\xi = 0.75$)

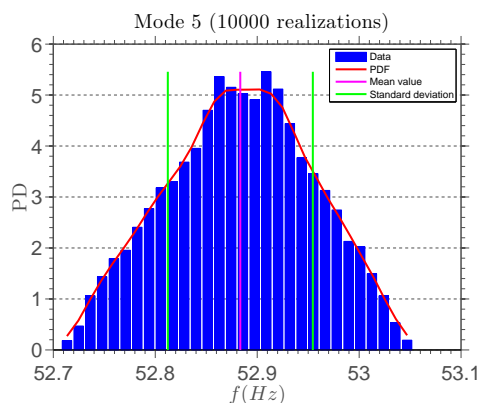


Figure 11: PDF - 5th natural frequency (calcul. param.)

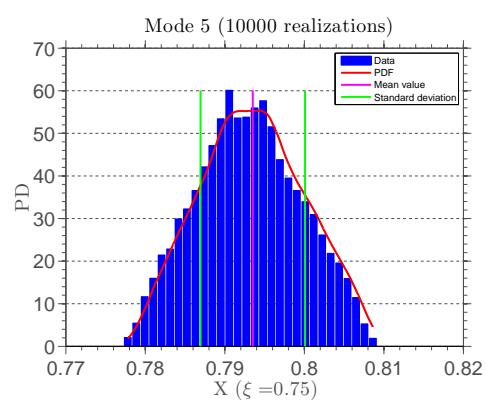
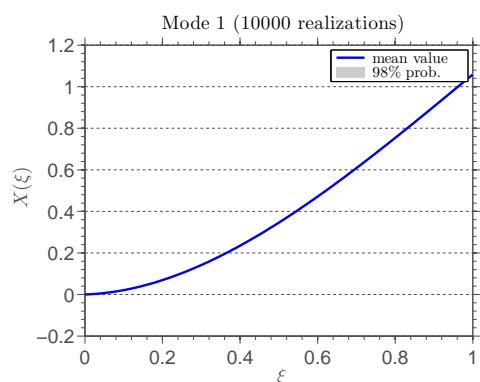
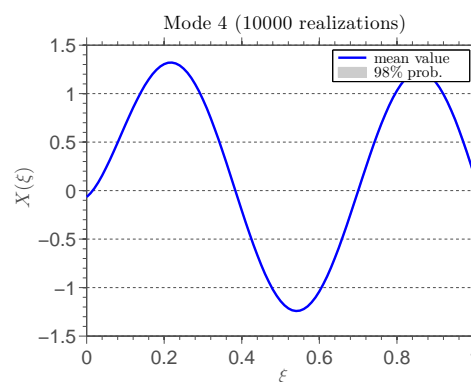
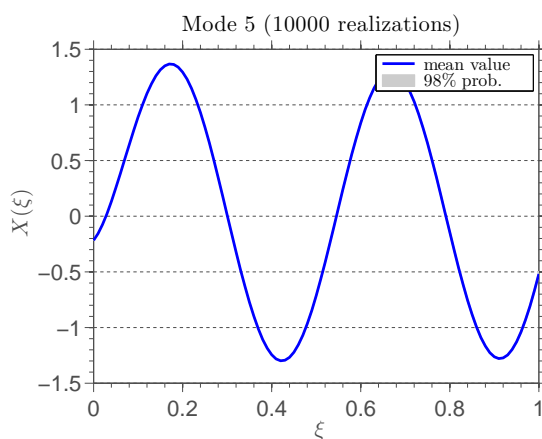


Figure 12: PDF - 5th mode ($\xi = 0.75$)

Figure 13: 1st modeFigure 14: 4th modeFigure 15: 5th mode

Method	Mode nbr.	Time	Mean nat.freq. (Hz)	Std. dev. (Hz)
MC	1	90 s	0.4564	$9.9e^{-4}$
MC	4	10 min	32.79	$5.0e^{-2}$
MC	5	11 min	56.27	0.23
Colloc.	1	150 s	0.4564	$9.9 \cdot 10^{-4}$

Table 2: Performance for MC and Collocation

For solving random problems under the non-intrusive manner, in each realization, the problem is solved deterministically, then, it is effective to compare first, deterministic results. The Table 3 shows the results found for natural frequencies using approach A and B. Those values were obtained considering that $E\{X_{\eta_l}\} = \eta_l = 40.02$ and $E\{X_{\eta_r}\} = \eta_r = 5935$ (all other parameters from Table 1 are deterministic). The values shown represent the results for 3 modes and for two configurations of tower placement: 1 - fixed at the ground without lumped mass at the top and, 2 - with two springs (translational and rotational) at the base with lumped mass at the top. The case (1) is the simplest and the results for this case is in the second column of the first block of the Table 3. They are in accordance to those from the literature. The results in the

Natural frequencies (Hz) - (Fixed at the bottom w/o lumped mass)		
-	Strong formul.	Fin. elem. formul.
Mode 1	1.1387	1.1370
Mode 4	39.1565	39.8078
Mode 5	64.7285	64.5987
Natural frequencies (Hz) - (Springs at the bottom w. lumped mass)		
-	Strong formul.	Fin. elem. formul.
Mode 1	0.4525	0.4575
Mode 4	31.5869	31.5433
Mode 5	52.8828	52.3503

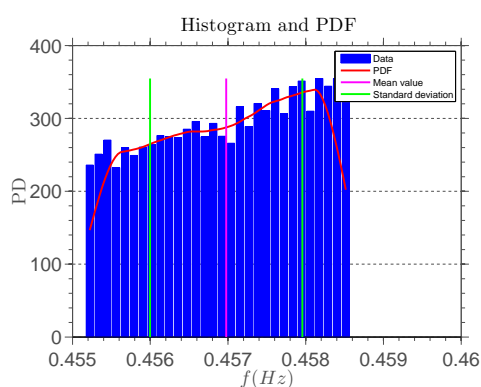
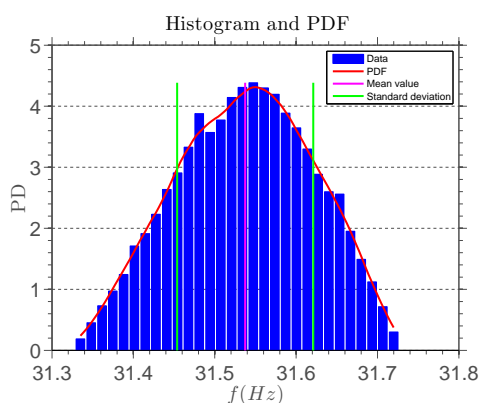
Table 3: Comparison - deterministic results

second column (from finite element formulation) diverge a little bit but in all cases the error is less that 2% if compared to the values from the left column.

In Table 3 using approach B, the number of elements to reach the precisions of $1 \cdot 10^{-3}$ was 80.

For random evaluations with the approach B, first, the program calculates a certain number of natural frequencies and modes within a required precision (in the present case, 0.01). Then, one specific value of the natural frequency is chosen together with its correspondent modal function. Stochastic simulations are carried out and statistics are made to determine mean values and standard deviations.

The number of simulations was 10000. The number of elements necessary to give the first mode with a precision of 0.01 was 40, for all modes. The graphs for distribution of natural frequency for both modes are presented in Figures 16 and 17.

Figure 16: PDF - 1st natural frequencyFigure 17: PDF - 4th natural frequency

About 3.5 minutes were spent to create each data set presented in graphs 16 and 17. In the first, the mean value is (0.457) Hz and the standard deviation is $1 \cdot 10^{-3}$. For the second, the 4th mode, the mean value and standard deviation are respectively, 31.5377(31.54) Hz and $9 \cdot 10^{-2}$ Hz. These results are quite similar to those from Table 3 but not equal and the error is about 1.1% for the first and 0.2% for the second. Increasing the precision to 0.001 the results are almost the same but the number of elements rises to 80. In this case, the mean value is

31.5375(31.54) Hz. The standard deviation is the same. The difference between both mean values is in the order of $1 \cdot 10^{-4}$, irrelevant, considering the variation of the mean. On the other hand, if the results are compared absolutely, the difference between mean values for the higher mode is about 0.05 Hz, but considering that the standard deviation for each result is about 0.1 Hz, this shows some incompatibility.

5 CONCLUSIONS

In this paper two modeling approaches for modal analysis of wind tower were presented. On the one hand, variational formulation, which can be solved with finite element discretization and on the other hand, strong formulation, simplified in order to permit an exact analytical solution. Furthermore, the model has been extended to a stochastic description, so that input uncertainties could be considered. Analysis of variance was used to determine that the stiffnesses associated to foundation characteristics (rotational and lateral) has strong influence on the dynamic behavior. Some simulations of a wind tower were performed under the assumption that two parameters associated to the foundation, η_r and η_l , have random behavior under uniform density of probability. Nevertheless, those two uncertain soil parameters cause only a small variation in natural frequency and by consequence, in the form of the modes.

Also, the different simulation methods were compared. The results for the Monte Carlo method were equal to the one with the stochastic collocation method but the latter showed better performance in convergence speed.

Next improvements in this work will be its extension to consider other parameters variation (geometrical and constitutive) and incorporation of torsional modes as well.

REFERENCES

- Adhikari S. and Battacharya S. Dynamic analysis of wind turbine towers on flexible foundations. *Shock and Vibration*, 19:37–56, 2012.
- Gerstner T. and Griebel M. Dimension-adaptive tensor-product quadrature. *Computing*, 71:65–87, 2003.
- Harzheim L. *Strukturoptimierung: Grundlagen und Anwendungen*, volume 1. Verlag Harri DeutschSpringer, 2008.
- HeidelbergCementAG. *Betontechnische Daten*. HeidelbergCement AG, 2011.
- Inman D. *Engineering Vibration*, volume 1. Prentice Hall PTR, NJ, USA, 2003.
- Jeong S., Murayama M., and Yamamoto K. Efficient optimization design method using kriging model. *AIAA paper 2004*, 2004.
- Jones D., Schonlau M., and Welch W. Efficient global optimization of expensive black-box functions. *Journal of Global Optimization*, 13:455–492, 1998.
- Le Maître O. and Knio O. *Spectral Methods for Uncertainty Quantification. With Application to Computational Fluid Dynamics*. Springer, 2010.
- Meirovitch L. *Principles and Techniques of Vibrations*. Prentice-Hall International, Inc., New Jersey, 1997.
- Schieche B. *Unsteady Adaptive Stochastic Collocation Methods on Sparse Grids*, volume 1. Dr. Hut, München, 2012.
- Schöwer R. *Das Baustellenhandbuch der Masstoleranzen*, volume 7. Forum, 2013.
- Tempel D. and Molenaar D.P. Wind turbine structural dynamics - a review of the principles for modern power generation, onshore and offshore. *Wind Engineering*, 26:211–220, 2002.
- Wu J. and Hsu S. A unified approach for the free vibration analysis of an elastically supported

immersed uniform beam carrying an eccentric tip mass with rotary inertia. *Journal of Sound and Vibration*, 291:1122–1147, 2006.